Luminosity Functions and Star Formation Rates at $z \sim 6 - 10$: Galaxy Buildup in the Reionization Age

Rychard Bouwens and Garth Illingworth
Department of Astronomy, University of California, Santa Cruz

Abstract. HST ACS and NICMOS data are now of sufficient depth and areal coverage to place strong constraints on the formation and evolution of galaxies during the first 1-2 Gyrs of the universe. Of particular interest are galaxies at $z \sim 6$ since they represent the earliest epoch accessible to current high-efficiency optical instrumentation. To this end, we have constructed a sample of 506 $z \sim 6$ objects from all the deepest wide-area HST data (UDF, UDF-Parallel, and GOODS fields). They have been used to construct an optimal determination of the rest-frame continuum UV LF at $z \sim 6$. Our LF extends to over 3 magnitudes below L^*, fainter than has been done at $z \sim 3$. Over the interval $z \sim 6$ to $z \sim 3$, we find strong evidence for evolution in the UV LF. Though constraints on the faint-end slope remain modest (and are consistent with no-evolution), the characteristic luminosity appears to have approximately doubled over the interval $z \sim 6$ to $z \sim 3$, consistent with hierarchical expectations. Remarkably, this shift to lower luminosities extends to even higher redshifts. Using all deep $J + H$ NICMOS observations (800 orbits in total), we have been able to demonstrate that the bright end of the LF ($> 0.3L^*_{z=3}$) is at least 5 times lower at $z \sim 10$ than at $z \sim 4$, with a similar deficit being established from our recent detections and first statistical sample of $z \sim 7 - 8$ galaxies using our UDF NICMOS data. In these proceedings, we discuss what is known about the UV LF and UV luminosity density at $z \sim 6 - 10$ from current data and its evolution relative to $z \sim 3$. We also describe several exciting prospects for advance in this area over the next year.

1 Introduction

Great progress has been made over the past few years in our observational understanding of galaxies at the end of the first billion years of the universe. Much of this progress has come at $z \sim 3 - 6$ and has been due in large part to the substantial gains in surveying efficiency made in the optical by the Advanced Camera for Surveys (ACS) on HST. This instrument provides us with a nearly $\sim 10\times$ increase in optical imaging efficiency over what was available with WFPC2, higher resolution imaging, and a reasonably efficient, red z-band filter. Putting together these capabilities with the well-established dropout technique (e.g., [27]), it became possible to select literally hundreds to thousands of galaxies at redshifts of $z \sim 3 - 6$ [5, 17].

2 $z \sim 6$ Rest-Frame Continuum UV LF

Experience over the past two years has shown that a simple $i - z > 1.3$ color selection is remarkably effective at isolating galaxies at $z \sim 6$ [24, 3, 14]. Though a small fraction of the selected sources are found to be low mass stars and low-redshift galaxies, most of these contaminants can be eliminated by making some requirement on their stellarity (i.e., how pointlike they are) or their flux in a bluer band (e.g., the V_{606}-band). These results have now been verified spectroscopically down to $z_{850,AB} \sim 27.5$ [18, 25, 15].

With this increasing understanding of the i-dropout selection, different studies attempted to construct rest-frame continuum UV ($\sim 1350\mathring{A}$) luminosity functions (LFs) at $z \sim 6$ [4, 11, 29, 18]. Despite small differences in detail, each of these studies find that there were significantly fewer galaxies at $z \sim 6$ (per volume element) than at $z \sim 3$. A recent determination of this LF by our team is shown in Figure 2a and incorporates the results from some ~ 510 i-dropouts selected from the two GOODS fields (enhanced to include the SNe search data – to be GOODS v2.0), two ACS parallel fields to the UDF, and the UDF [10]. For comparison, we have also plotted the $z \sim 3$ LF [28], and it is amazing to note that the $z \sim 6$ LF extends fainter than at $z \sim 3$, demonstrating the remarkable surveying efficiency of current optical instrumentation. It is also evident that our $z \sim 6$ LF shows a much larger deficit at the bright end than at the faint end, suggesting that higher redshift galaxies are of much lower luminosity (on average). This explains (at least in part) why early searches down to brighter limiting magnitudes [24] found more substantial evolution than similar searches down to fainter magnitudes [3, 17].

We can look at this evolution more quantitatively. In Figure 2b, we plot the likelihood contours for the $z \sim 6$ LF and contrast it with the equivalent values at $z \sim 3$ (thick black cross). The red shaded regions on this plot indicate those values of α and M^*_{UV} which are ruled out at 95% confidence using the current HST data. Though the constraints on the faint-end slope α at $z \sim 6$ are still somewhat modest, the preferred values for the characteristic luminosity M^*_{UV} are much fainter than at $z \sim 3$, suggesting that there has been evolution

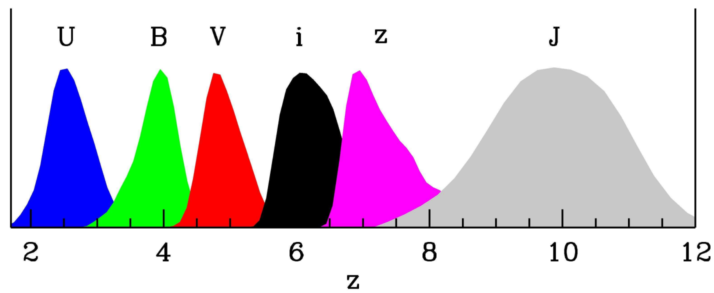

Figure 1: Estimated redshift distributions for fairly generic U, B, V, i, z, and J-dropout selections. The standard suite of HST bands (e.g., F300W, F435W, F606W, F775W, F850LP, F110W) are used for these selections.

in the characteristic scales on which star formation is occurring. This provides us with one of our first, most direct evidences for the hierarchical buildup of galaxies early in the history of the universe (see also [14] and [29]). Further refinements to the $z \sim 6$ LF should be forthcoming over the next year due to the availability of two additional deep fields to be taken with ACS (GO-10632).

3 First Detections of $z \sim 7-8$ Galaxies

Extending the dropout search beyond $z \sim 6$ requires the detection of objects in the infrared. This has been difficult due to the well-known limitations of infrared technology and because $z \sim 7-8$ objects are likely to be very faint. At $z \sim 6$, the characteristic luminosity is nearly 0.7 mags fainter than at $z \sim 3$. Extrapolated to even higher redshift, these luminosities should be even fainter still, perhaps $0.3\ L^*_{z=3}$. In the H-band, this corresponds to a magnitude of 27.3, which can only be reached in deep NICMOS studies and very deep ground-based studies around massive lensing clusters.

The deep NICMOS imaging over the optical UDF provided us with one of our first opportunities to find $z \sim 7-8$ galaxies. The 5σ limiting depths in these data were 27.6 in the J_{110}-band and 27.4 in the H_{160}-band. Moreover, the optical data for this field were more than sufficient to set strong constraints on the z_{850}-band fluxes. Using a relatively aggressive set of detection criteria, we carried out a z_{850}-dropout selection on these data and found 5 $z \sim 7-8$ candidates. Successive tests on our selection–including scattering experiments and selection on the negative images–suggested that most of our 5 candidates were likely at $z \sim 7-8$ and there was only one contaminant. We therefore adopted as our likely sample 4 fiducial candidates.

To assess the implications of this first statistical sample of $z \sim 7-8$ objects, we generated no-evolution predictions based upon a lower redshift $z \sim 3.8$ B_{435}-dropout sample[8] using our well-established cloning machinery [1, 2, 9]. An important consideration in projecting these lower redshift samples to high redshifts was the observed evolution in size [16, 5] and UV color [26, 10]. Running through these simulations, we estimated that 14 objects would be found (if there was no-evolution from $z \sim 3.8$). We compared this prediction with our 4 fiducial z-dropout candidates, given the expected small but non-zero contamination. This suggested that the rest-frame UV ($\sim 1600 \mathring{A}$) luminosity density at $z \sim 7-8$ was just $0.28\times$ that at $z \sim 3.8$ (number weighted) or $0.20\times$ the $z \sim 3.8$ value (if we use a luminosity weighting).

Though a first estimate of the rest-frame UV luminosity density at $z \sim 7-8$, our determination still suffered from some substantial uncertainties, notably the Poissonian errors ($\pm 50\%$), cosmic variance (factor of 2), as well as the overall contamination level ($\sim 0-2$ objects). This situation should improve substantially over the next year using data from two HST programs: (1) a deep z_{850}-dropout search in the field (GO-10632) and (2) a similar search around seven massive lensing clusters (GO-10504 and GO-10699). Both should yield $\sim 5-10$ $z \sim 7-8$ candidates, substantially reducing uncertainties from our previously quoted estimates based on the HUDF NICMOS footprint. Simultaneously, searches with large ground-based telescopes are ongoing and have yielded a sizeable number of candidates, particularly around lensing clusters [21, 22].

4 Searches for $z \sim 10$ Galaxies

The detection and confirmation of galaxies at $z \sim 10$ appears to be significantly more difficult than even at $z \sim 7-8$. Though the additional distance plays a small role, by far the biggest challenge is their luminosity: $z \sim 10$ galaxies are expected to have very low luminosities, several times lower than at $z \sim 6$ or $z \sim 7-8$ [12, 13]. Even assuming no evolution in luminosity from $z \sim 7-8$ to $z \sim 10$, typical magnitudes for these objects would be $\sim$28 in the H-band, suggesting that one would need to probe to very faint magnitudes indeed.

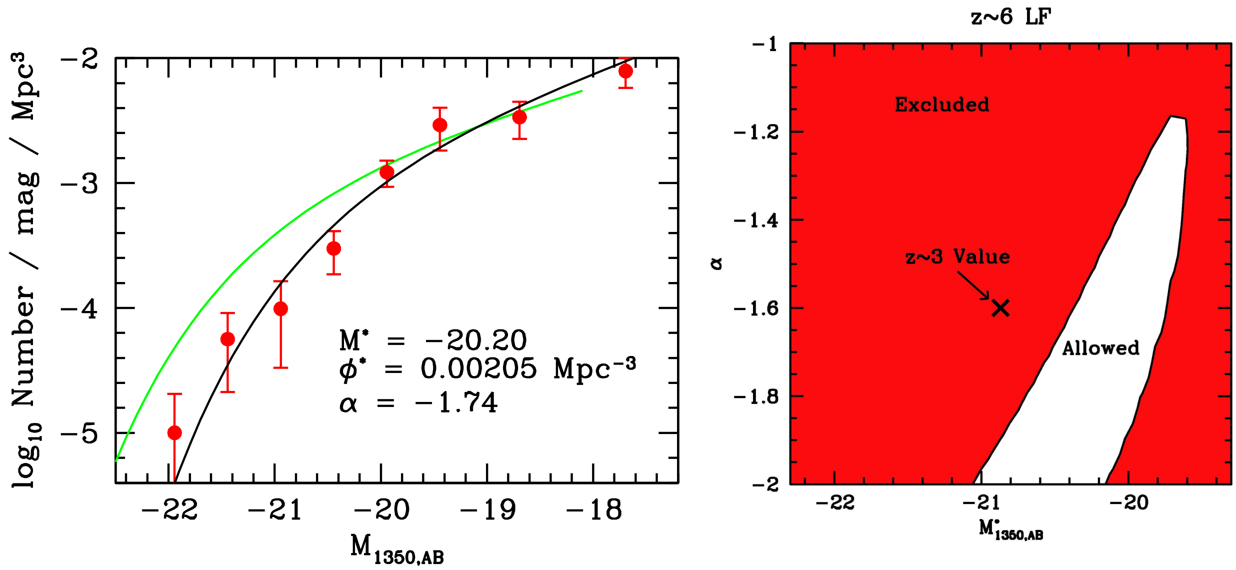

Figure 2: *(left panel).* The rest-frame continuum *UV* ($\sim 1350\mathring{A}$) LF estimated from the UDF, the UDF-Ps, and the GOODS fields, shown in terms of the best-fit stepwise parameterizations (*red circles* with 1σ errors) and Schechter function (*solid black line*)[10]. The $z \sim 3$ LF is shown for comparison (*thick green line*) [28]. Our $z \sim 6$ LF shows a clear turnover at the bright end relative to the $z \sim 3$ LF and suggests that there has been a shift in the characteristic luminosity from $z \sim 6$ to $z \sim 3$. *(right panel).* The allowed regions of parameter space (95% confidence) for the $z \sim 6$ LF using current HST data [10]. The equivalent $z \sim 3$ values are shown with the large black cross. Though only modest constraints are possible on the $z \sim 6$ faint-end slope α, the characteristic luminosity at $z \sim 6$ appears to be ~ 0.7 mags fainter than at $z \sim 3$.

One way of reaching such magnitudes is to use the very deep IR imaging capabilities of the HST NICMOS camera. Unfortunately, even with this instrument, searches for $z \sim 10$ objects are still extremely expensive, e.g., ~ 150 orbits are needed to detect just one $z \sim 10$ object, and this assumes that the UV LF does not evolve from $z \sim 10$ to $z \sim 6$. It is thus no surprise that there has been a lack of dedicated searches. Nevertheless, it is possible to take advantage of the deep J_{110} and H_{160} parallel data associated with several HST deep fields to conduct a search. Such data is available for the HDF-S (150 orbits) and the UDF ($\sim$340 orbits). There is also deep NICMOS J+H imaging over the WFPC2 HDF-N (176 orbits) and a portion of the ACS UDF (144 orbits). The 5σ limiting magnitudes of these data range from $H_{160,AB} \sim 27$ to $H_{160,AB} \sim 28.5$, which is sufficient to identify $z \sim 10$ galaxies down to $0.3L^*_{z=3}$.

To see what we could learn from these data, we carried out a search for $(J_{110} - H_{160})_{AB} > 1.8$ J-dropouts and found 11 objects [7]. We eliminated those objects with 2σ detections in the optical bands or with $H - K$ colors substantially redder than the typical starburst type object (i.e., UV continuum slopes $\beta > 0.5$). This left us with 3 candidates, all of which are in the NICMOS parallel fields to the UDF. Since we did not have comparably deep images blueward or redward of the $J_{110}H_{160}$ passbands, it was difficult for us to be very sure about the redshifts of our 3 candidates. Nevertheless, we could still compare these 3 candidates with the numbers expected assuming no-evolution from $z \sim 6$. Repeating the simulations described in §3, we estimated that 4.8 J_{110}-dropouts would be found, only somewhat higher than our 3 candidates. If we assume that all three candidates were at $z \sim 10$, the normalization we would obtain for the $z \sim 10$ LF is just $0.7 \pm 0.3\times$ that at $z \sim 6$. On the other hand, assuming that none of these candidates were at these redshifts, the normalization we would obtain is just $< 0.2\times$ the $z \sim 6$ value (1σ). Remarkably, we found that these results were not very sensitive to cosmic variance ($\sim 19\%$ RMS). This is due to the extremely large comoving distances probed in J-dropout searches (~ 500 Mpc).

The current round of HST proposals should strengthen these constraints significantly. Not only will we increase the total NICMOS observing time relevant to these searches by $\sim 60\%$ (improving the statistics), but we will obtain some very deep ACS observations (~ 28.5 mag at 5σ for apertures that match the NICMOS data) over the deep NICMOS parallels containing our 3 $z \sim 10$ candidates. Independent searches are also ongoing around lensing clusters (GO-10380, GO-10504, GTO-10699, and [22]), and we note that there are claims by some teams to have a very good set of candidates.

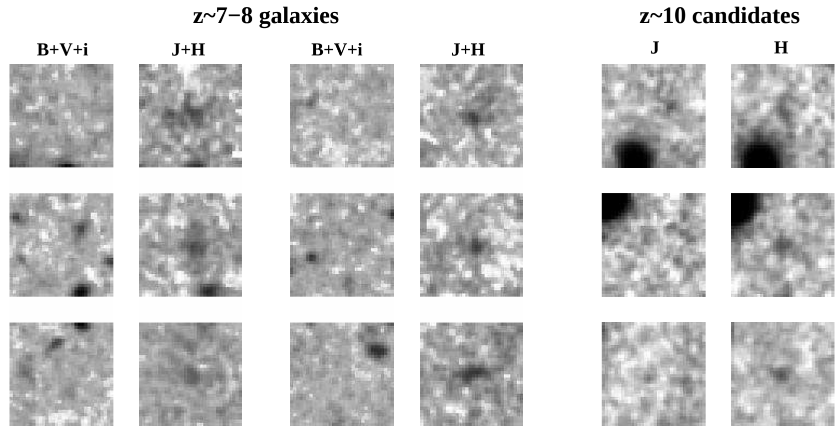

Figure 3: Candidate $z \sim 7-8$ and $z \sim 10$ galaxies from the UDF NICMOS footprint and NICMOS parallels to the UDF [6, 7].

5 Summary

Current observations are now of sufficient quality to robustly determine the rest-frame UV (~ 1350Å) luminosity function at $z \sim 6$. These determinations extend to nearly three magnitudes below L^*, fainter than has been possible at $z \sim 3$, demonstrating the efficiency of current optical technology. Substantial changes are evident in the LF relative to $z \sim 3$, suggesting that typical galaxies have more than doubled their star formation rates over this interval. The observed evolution is suggestive of that expected from popular hierarchical models, and would seem to indicate that we are literally witnessing the buildup of galaxies over this range.

Progress with higher redshift dropout samples has been less dramatic, but is still forthcoming. Our sample of $z \sim 7-8$ z_{850}-dropouts in the HUDF provided our first statistical sample of galaxies in this epoch and thus allowed an initial estimate of the luminosity density[6]. Searches for higher redshift $z \sim 10$ J-dropouts have resulted in some candidates as well as yielding some useful upper limits on the bright end of the UV LF [7]. Galaxies at both times stand to undergo substantial improvements as the result of future and ongoing programs. Of course, for truly substantial gains in this area, we will need to wait for the availability of high resolution, high sensitivity space-based imagers, such as WFC3 or NIRCam (JWST).

Acknowledgements. We are indebted to the many members of the ACS GTO and UDF NICMOS GO teams for their contribution to the current research. Of particular note was the assistance provided by John Blakeslee, Daniel Eisenstein, Marijn Franx, Rodger Thompson, and Pieter van Dokkum, each of whom contributed in an extremely important way. We also acknowledge valuable discussions with Brandon Allgood, Tom Broadhurst, Andy Bunker, Akio Inoue, Sangeeta Malhotra, James Rhoads, Evan Scannapieco, Daniel Schaerer, and Jason Tumlinson. ACS was developed under NASA contract NAS5-32865, and this research was supported under NASA grant HST-GO09803.05-A and NAG5-7697.

References

[1] R.J. Bouwens, et al. Astroph. J. **506**, 557 (1998).

[2] R.J. Bouwens, et al. Astroph. J. **593**, 640 (2003a).

[3] R.J. Bouwens, et al. Astroph. J. **595**, 589 (2003b).

[4] R.J. Bouwens, et al. Astroph. J. Letters **606**, L25 (2004a).

[5] R.J. Bouwens, et al. Astroph. J. Letters **611**, 1 (2004b).

[6] R.J. Bouwens, et al. Astroph. J. Letters **616**, L79 (2004c).

[7] R.J. Bouwens, et al. Astroph. J. Letters **624**, L5 (2005a).

[8] R.J. Bouwens, et al. Astroph. J., submitted (2005b).

[9] R.J. Bouwens, et al. Astroph. J., submitted (2005c).

[10] R.J. Bouwens, et al. Astroph. J., in press (2005d), astro-ph/0509641.

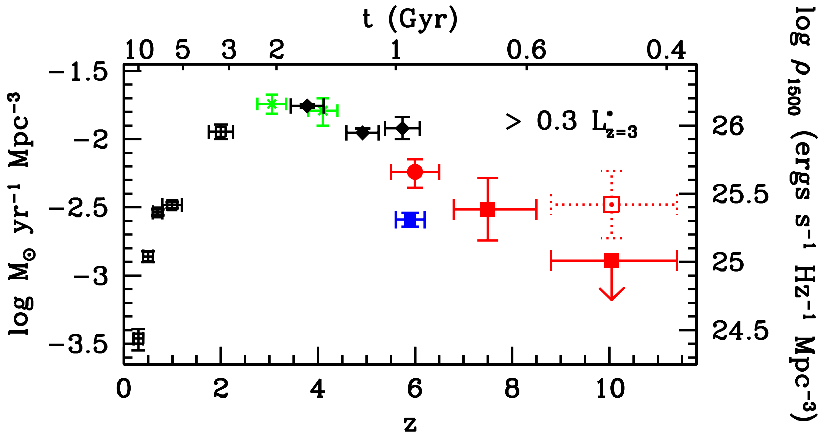

Figure 4: The cosmic star formation rate density versus redshift with no extinction correction. The star formation rate density (integrated down to 0.3 $L^*_{z=3}$ – the limit of our $z \sim 7-8$ and $z \sim 10$ searches) was calculated from the luminosity density in the rest-frame UV continuum ($\sim 1500\AA$: plotted on the right vertical axis) using canonical assumptions and a Salpeter IMF [20]. The open red square at $z \sim 10$ shows our result if 3 objects from this study prove to be at $z \sim 10$, while the large downward pointing arrow shows our 1σ limits if none are [7]. Included on this plot are also estimates by [23] (open black squares), [28] (green crosses), [17] (black diamonds), [11] (solid blue square), [6] (solid red square), and [10] (solid red circle).

[11] A.J. Bunker, 2004, *MNRAS* **355**, 374 (2004)

[12] A. Cooray, *MNRAS*, submitted, astro-ph/0506087 (2005).

[13] R. Davé, this meeting (2005).

[14] M. Dickinson, et al. Astroph. J. Letters **600**, L99 (2004).

[15] C. Dow-Hygelund, et al. Astroph. J. Letters **630**, L137 (2005).

[16] H.C. Ferguson, et al. Astroph. J. Letters **600**, L107 (2004).

[17] M. Giavalisco, et al. Astroph. J. Letters **600**, L103 (2004).

[18] S. Malhotra, et al. Astroph. J. **626**, 666 (2005).

[19] H.J. Mo, et al. *MNRAS* **295**, 319 (1998)

[20] P. Madau, et al. *MNRAS* **498**, 106 (1998)

[21] F. Mannucci, et al., in preparation (2005).

[22] J. Richard, et al. Astron. & Astroph., submitted (2005).

[23] Schiminovich, D., et al. Astroph. J. Letters **619**, 47 (2005).

[24] E.R. Stanway, et al. *MNRAS* **342**, 439 (2003)

[25] E.R. Stanway, et al. AstroPh. J. Letters **604**, L13 (2004).

[26] E.R. Stanway, et al. *MNRAS* **359**, 1184 (2005).

[27] C.C. Steidel, et al. Astroph. J. Letters **462**, L17 (1996).

[28] C.C. Steidel, K.L. Adelberger, M. Giavalisco, M. Dickinson, M. Pettini. Astroph. J. **519**, 1 (1999).

[29] H. Yan & R.A. Windhorst Astroph. J. Letters **612**, L93 (2004).